Available online at www.sciencedirect.com

ScienceDirect

Journal of the Nigerian Mathematical Society 35 (2016) 66–81

Journal of the Nigerian Mathematical Society

www.elsevier.com/locate/jnnms

Effects of diffusion-thermo and thermo-diffusion on two-phase boundary layer flow past a stretching sheet with fluid-particle suspension and chemical reaction: A numerical study

K.L. Krupa Lakshmi[a], B.J. Gireesha[a,b,*], Rama.S.R. Gorla[b], B. Mahanthesh[a,c]

[a] *Department of Studies and Research in Mathematics, Kuvempu University, Shankaraghatta-577 451, Shimoga, Karnataka, India*
[b] *Department of Mechanical Engineering, Cleveland State University, Cleveland-44114, OH, USA*
[c] *Department of Mathematics, AIMS Institute of Higher Education, Peenya-560058, Bangalore, India*

Received 25 August 2015; accepted 29 October 2015
Available online 27 November 2015

Abstract

A numerical investigation on laminar boundary layer flow, heat and mass transfer of two-phase particulate suspension induced by a linearly stretching sheet is carried out. In the mathematical formulation both the fluid and particle phases are treated as two separate interacting continua. The effects of magnetic field, diffusion-thermo, thermal-diffusion, thermal radiation and first order chemical reaction are taken into the account. The relevant governing partial differential equations corresponding to the momentum, energy and concentration are transformed into a system of non-linear ordinary differential equations with the help of appropriate similarity transformations and then solved numerically using Runge–Kutta-Fehlberg fourth fifth order method along with shooting scheme. The effects of the relevant physical parameters on the flow, heat and mass transfer characteristics of both fluid and particle phases were numerically obtained and discussed in detail. It is found that, the momentum, thermal and solute boundary layer thickness decreases with increasing the particles loading.

Keywords: Heat and mass transfer; Stretching sheet; Soret effect; Dufour effect; Numerical solution; Fluid-particle suspension

1. Introduction

The study of heat and mass transfer due to a stretching surface is of great practical importance to engineers and scientists because of its occurrence in many branches of science and engineering. It plays an important role in several engineering applications and manufacturing processes in the industry such as, aerodynamic extrusion of plastic sheets, manufacturing and rolling of plastic films, cooling of metal sheets and etc. Sakiadis [1] presented the pioneering work

Peer review under responsibility of Nigerian Mathematical Society.
* Corresponding author at: Department of Studies and Research in Mathematics, Kuvempu University, Shankaraghatta-577 451, Shimoga, Karnataka, India.
E-mail addresses: krupa.lakshmi@yahoo.com (K.L. Krupa Lakshmi), g.bijjanaljayanna@csuohio.edu (B.J. Gireesha), r.gorla@csuohio.edu (R.S.R. Gorla), bmanths@gmail.com (B. Mahanthesh).

http://dx.doi.org/10.1016/j.jnnms.2015.10.003

on the boundary layer flow past a continues moving surface with a constant velocity. He formulated the boundary layer equations for two dimensional and symmetric flows. Crane [2] discussed boundary layer flow caused by the stretching of elastic flat surfaces under various physical situations. Grubka and Bobba [3] have worked on the heat transfer occurring on a linearly stretching surface under variable temperature.

The mass transfer caused by the temperature gradient is called Soret effect (thermal diffusion), while the heat transfer caused by the concentration gradient is called Dufour effect (diffusion-thermo). The Soret effect is utilised for isotope separation and in a mixture between gases with very light molecular weight and of medium molecular weight. The importance of Soret and Dufour effects for fluids has been investigated by Dursunkaya and Worek [4], Anghel and Takhar [5] and Postelnicu [6]. Hayat et al. [7] developed analytical solutions for Soret and Dufour effects on mixed convection boundary layer flow over a stretching vertical surface in a porous medium filled with viscoelastic fluid. Beg et al. [8] numerically investigated the free convection magnetohydrodynamic heat and mass transfer from a stretching surface to a saturated porous medium with Soret and Dufour effects. Aziz [9] addressed the thermal-diffusion and diffusion-thermo effects on combined heat and mass transfer by hydromagnetic three-dimensional free convection over a permeable stretching surface. Pal and Chatterjee [10] discussed the mixed convection heat and mass transfer past a stretching surface in a micropolar fluid saturated porous medium under the influence Soret and Dufour effects. Makinde and Olanrewaju [11] studied the mixed convection with Soret and Dufour effects past a porous plate moving through a binary mixture of fluid. Recently, the same authors [12] have investigated the effects of thermal diffusion and diffusion thermo on MHD boundary layer flow of heat and mass transfer past a moving vertical plate.

Chemical reactions can be categorised as either homogeneous or heterogeneous processes. These reactions mainly depend on whether they occur in an interface or as a single phase volume reaction. Homogeneous reaction is one that occurs uniformly through a given phase whereas a heterogeneous reaction takes place in a restricted region or within the boundary of a phase. In a first order reaction, the rate of reaction is directly proportional to the concentration. In many chemical engineering processes, a chemical reaction between a foreign mass and the fluid does occur. These processes take place in various industrial applications, such as production of polymer, manufacturing of ceramics or glassware, food processing and so on. Therefore, the study of heat and mass transfer with chemical reaction effect is given primary importance in chemical and hydrometallurgical industries.

Pal and Mondal [13] theoretically investigated the effects of chemical reaction on MHD non-Darcian mixed convective heat and mass transfer over a linear stretching sheet. Further, they have analysed the chemical reaction effect on heat and mass transfer over a non-linear stretching sheet [14]. The problem of free convection heat and mass transfer over a porous stretching surface in the presence of chemical reaction has been studied by Kandasamy et al. [15]. The influence of chemical reaction on heat and mass transfer by natural convection from vertical surfaces in a porous media with Soret and Dufour effects was numerically investigated by Postelnicu [16]. The investigations dealing with chemical reaction effect on fluid flow with different physical conditions can be found in the works of Das [17], Mansour et al. [18], Makinde et al. [19], Chamkha and EL-Kabeir [20] and Gireesha et al. [21].

The previously mentioned articles are concerned with single-phase flow analysis. The heat and mass transfer of fluid-particle mixture is a subject which attracted many investigators due to its application in many engineering and natural processes. These include environmental and atmospheric pollution, nuclear reactor safety, filtration, sedimentation of particles on gas turbine blades, particulate deposition on semi-conductor wafers in the electronic industry and others. Its relevance is also seen in gas cooling systems, fluidized beds, combustion, crude oil purification, electrostatic precipitation, polymer technology, transport processes and petroleum industry. In view of these applications, Saffman [22] was the first who formulated the governing equations for dusty fluid and has studied the stability of the laminar flow of a dusty gas. Later on, mathematical analysis based on the continuum approach for steady laminar boundary layer flow and heat transfer of fluid-particle suspension with different aspects were developed by Chamkha [23,24]. The free-convection flow and heat transfer of two-phase flow over an infinite porous vertical plate was theoretically analyzed by Chamkha and Ramadan [25]. They have developed analytical solutions and found that an increase of particle loading results in a retardation of momentum of both fluid and particle phases. Vajravelu and Nayfeh [26] have addressed the hydromagnetic flow of a dusty fluid over a stretching sheet. Makinde and Chinyoka [27] presented numerical results for MHD transient flow and heat transfer of a dusty fluid in a channel with variable physical properties and Navier slip condition. Attia et al. [28] have studied the ion slip effect on the unsteady Couette flow and heat transfer of a dusty fluid in the presence of uniform suction and injection. Recently, Gireesha et al. [29–31] have studied the fluid-particle suspension over a stretching surface with different physical conditions.

The present work is undertaken in order to study the heat and mass transfer of a dusty fluid with Soret and Dufour's effect on boundary layer flow over a stretching surface. The novelty of this study is that Soret, Dufour and chemical reaction effects are included in the heat and mass transfer analysis of the two-phase fluid-particle suspension. The numerical solution is obtained for the governing equations of conservation of momentum, temperature and concentration for both fluid and particle phases.

2. Mathematical formulation

Flow Analysis:

Consider a two dimensional, steady, laminar boundary layer flow of an incompressible, viscous, electrically conducting dusty fluid over a linearly stretching surface. According to the coordinate system, the x-axis is chosen parallel to the stretching surface and y-axis is taken normal to it. A uniform magnetic field B_0 is imposed along the y-axis. The fluid properties are assumed to be constant and the chemical reaction is assumed to take place in the flow. The dust particles are embedded in the fluid by using surface charge technology. The dust particles are assumed to be spherical in shape, equal in size and uniformly distributed throughout the fluid. The interparticle collision and volume fraction of dust particles are neglected. The magnetic Reynolds number is assumed to be small, so that the induced magnetic field is neglected. In addition, all fluid and particle properties are assumed to be constant. The fluid and dust particle motions are coupled only in the course of drag, heat and mass transfer between them. The Stokes linear drag theory is employed to model the drag force. The terms T_w and C_w represents the temperature and concentration of the fluid at the sheet which are higher than the ambient values T_∞ and C_∞ respectively. Using the above assumptions, the governing equations describing the conservation of mass and momentum for both fluid and particle phase can be written as follows [23,27]:

$$\frac{\partial u}{\partial x}+\frac{\partial v}{\partial y}=0, \tag{2.1}$$

$$\rho\left(u\frac{\partial u}{\partial x}+v\frac{\partial u}{\partial y}\right)=\mu\frac{\partial^2 u}{\partial y^2}+KN\left(u_p-u\right)-\sigma B_0^2 u, \tag{2.2}$$

$$\frac{\partial u_p}{\partial x}+\frac{\partial v_p}{\partial y}=0, \tag{2.3}$$

$$\rho_p\left(u_p\frac{\partial u_p}{\partial x}+v_p\frac{\partial u_p}{\partial y}\right)=KN\left(u-u_p\right), \tag{2.4}$$

where (u, v) and (u_p, v_p) are velocity components along x and y directions of fluid and dust particle phase respectively. ρ and ρ_p are density of the fluid and dust particles respectively. σ is the electrical conductivity of the fluid, μ-dynamic viscosity of the fluid, N-number density of dust particles, B_0-uniform magnetic field, $K=6\pi\mu r$ is the Stokes drag coefficient and r-radius of dust particle.

The boundary conditions for this problem can be written as:

$$\left.\begin{array}{lll} u=u_w, & v=0 & \text{at } y=0 \\ u\longrightarrow 0, & u_p\longrightarrow 0, \quad v_p\longrightarrow v & \text{as } y\longrightarrow\infty, \end{array}\right\} \tag{2.5}$$

where $u_w = bx$ is a the stretching sheet velocity and $b > 0$ is the stretching rate. Introduce the following transformations;

$$u=bxf'(\eta), \qquad v=-\sqrt{vb}\,f(\eta), \qquad \eta=\sqrt{\frac{u_w}{vx}}y$$

$$u_p=bxF'(\eta), \qquad v_p=-\sqrt{vb}F(\eta), \tag{2.6}$$

where a prime denote the differentiation with respect to η. It can be easily verified that the continuity Eqs. (2.1) and (2.3) are identically satisfied. Now, introducing the relation (2.6) into the Eqs. (2.2) and (2.4), we obtain the following nonlinear ordinary differential equations;

$$f'''(\eta)-\left[f'(\eta)\right]^2+f''(\eta)\,f(\eta)+l\beta_v[F'(\eta)-f'(\eta)]-M^2f'(\eta)=0, \tag{2.7}$$

$$F''(\eta)F(\eta) - \left[F'(\eta)\right]^2 + \beta_v[f'(\eta) - F'(\eta)] = 0, \tag{2.8}$$

where $l = Nm/\rho$ is the dust particles mass concentration parameter, $\tau_v = m/K$ is relaxation time of the dust particles i.e., the time required by a dust particle to adjust its velocity relative to the fluid, $\beta_v = 1/b\tau_v$ is fluid-particle interaction parameter and $M^2 = \sigma B_0^2/b\rho$ is magnetic parameter.
Using the transformations (2.6) into the boundary conditions (2.5) one can get;

$$\begin{aligned} &f'(\eta) = 1, \qquad f(\eta) = 0 \quad \text{at } \eta = 0, \\ &f'(\eta) \longrightarrow 0, \qquad F'(\eta) \longrightarrow 0, \qquad F(\eta) \longrightarrow f(\eta) \quad \text{as } \eta \to \infty. \end{aligned} \tag{2.9}$$

Heat Transfer Analysis:

The governing boundary layer heat transport equations for both fluid and particle phase are given by [23,27];

$$\rho C_p \left(u\frac{\partial T}{\partial x} + v\frac{\partial T}{\partial y}\right) = k\frac{\partial^2 T}{\partial y^2} + \frac{\rho_p C_m}{\tau_T}\left(T_p - T\right) + \frac{\rho_p}{\tau_v}\left(u_p - u\right)^2 - \frac{\partial q_r}{\partial y} + \frac{\rho D_m K_t}{C_s C_p}\frac{\partial^2 C}{\partial y^2}, \tag{2.10}$$

$$\rho_p C_m \left(u_p\frac{\partial T_p}{\partial x} + v_p\frac{\partial T_p}{\partial y}\right) = \frac{\rho_p C_m}{\tau_T}\left(T - T_p\right), \tag{2.11}$$

where T and T_p are the temperature of the fluid and dust particles respectively, C_p and C_m are the specific heat of fluid and dust particles respectively, τ_T-the thermal equilibrium time i.e., the time required by the dust cloud to adjust its temperature to that of fluid, k-thermal conductivity of the fluid, q_r- radiative heat flux, D_m is the diffusion coefficient, C_s is the concentration suseptability and K_t is the thermal diffusion ratio. According to the Rosseland diffusion approximation for radiation, q_r is given by;

$$q_r = -\frac{4\sigma^*}{3k^+}\frac{\partial T^4}{\partial y}, \tag{2.12}$$

where σ^*-Stefan–Boltzmann constant and k^+-mean absorption coefficient. It is noted that the optically thick radiation limit is considered in this model. Assuming that the temperature differences within the flow are sufficiently small such that T^4 may be expressed as a linear function of temperature, we expand T^4 in a Tayler series about T_∞ as follows,

$$T^4 = T_\infty^4 + 4T_\infty^3\left(T - T_\infty\right) + 6T_\infty^2\left(T - T_\infty\right)^2 + \ldots. \tag{2.13}$$

Neglect the higher order terms beyond the first degree in $(T - T_\infty)$, we can get;

$$T^4 \cong 4T_\infty^3 T - 3\,T_\infty^4. \tag{2.14}$$

Substituting Eq. (2.14) in Eq. (2.12) then,

$$\frac{\partial q_r}{\partial y} = -\frac{16\sigma^* T_\infty^4}{3k^*}\frac{\partial^2 T}{\partial y^2}. \tag{2.15}$$

In view of the Eq. (2.15), the energy Eq. (2.10) will becomes

$$\rho C_p \left(u\frac{\partial T}{\partial x} + v\frac{\partial T}{\partial y}\right) = \left(k + \frac{16T_\infty^4\sigma^*}{3k^*}\right)\frac{\partial^2 T}{\partial y^2} + \frac{\rho_p C_m}{\tau_T}\left(T_p - T\right) + \frac{\rho_p}{\tau_v}\left(u_p - u\right)^2 + \frac{\rho D_m K_t}{C_s C_p}\frac{\partial^2 C}{\partial y^2}. \tag{2.16}$$

Boundary conditions for the temperature are as follows;

$$\begin{aligned} &T = T_w = bx + T_\infty, \quad \text{at } y = 0, \\ &T \to T_\infty, \qquad T_p \to T_\infty, \quad \text{as } y \to \infty. \end{aligned} \tag{2.17}$$

The dimensionless fluid phase temperature $\theta(\eta)$ and dust phase temperature $\theta_p(\eta)$ are defined as:

$$\theta(\eta) = \frac{T - T_\infty}{T_w - T_\infty}, \qquad \theta_p(\eta) = \frac{T_p - T_\infty}{T_w - T_\infty}. \tag{2.18}$$

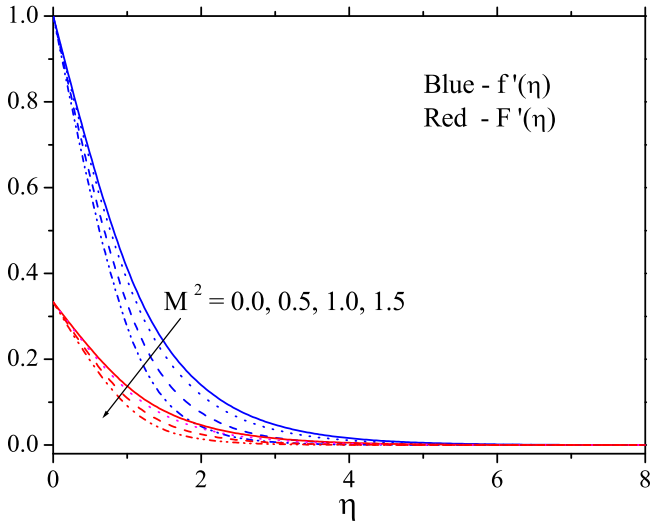

Fig. 1. The influence of M^2 on velocity profile.

Using (2.18) into (2.16) and (2.11), we obtain the following non-linear ordinary differential equations:

$$\left(1+\frac{4}{3}R\right)\theta''(\eta)+Pr\left\{\begin{array}{l}\theta'(\eta)\,f(\eta)-f'(\eta)\,\theta(\eta)\\ \quad+l\beta_T\gamma\left(\theta_p(\eta)-\theta(\eta)\right)\\ \quad+l\beta_v Ec\left[F'(\eta)-f'(\eta)\right]^2\end{array}\right\}+D_f\phi''(\eta)=0, \tag{2.19}$$

$$\theta_p'(\eta)\,F(\eta)-F'(\eta)\theta_p(\eta)-\beta_T\left[\theta_p(\eta)-\theta(\eta)\right]=0. \tag{2.20}$$

Corresponding boundary conditions are:

$$\begin{aligned}&\theta(\eta)=1, \quad \text{at } \eta=0\\ &\theta(\eta)\to 0, \qquad \theta_p(\eta)\to 0 \quad \text{as } \eta\to\infty\end{aligned} \tag{2.21}$$

where $Pr=\mu C_p/k$—Prandtl number, $Ec=u_w^2/C_p(T_w-T_\infty)$—Eckert number, $\gamma=C_m/C_p$—specific heat ratio, $\beta_T=1/b\tau_T$—fluid-particle interaction parameter for temperature, $R=4\sigma^*T_\infty^3/k^+k$—thermal radiation parameter and $D_f=D_mK_t(C_w-C_\infty)/C_sC_p(T_w-T_\infty)$—the Dufour number.

Mass Transfer Analysis:

The conservation mass equation for both fluid and dust phase are given by;

$$u\frac{\partial C}{\partial x}+v\frac{\partial C}{\partial y}=D_m\frac{\partial^2 C}{\partial y^2}+\frac{\rho_p}{\rho\tau_C}\left(C_p-C\right)+\frac{D_mK_t}{T_m}\frac{\partial^2 T}{\partial y^2}-K^*(C-C_\infty), \tag{2.22}$$

$$u_p\frac{\partial C_p}{\partial x}+v_p\frac{\partial C_p}{\partial y}=\frac{1}{\tau_c}\left(C-C_p\right), \tag{2.23}$$

where C and C_p are concentration species of the fluid and particle phase, D_m is the mass diffusivity coefficient, τ_C is the time required by a dust particle to adjust its concentration relative to the fluid and K^* is the chemical reaction co-efficient.

The relevant boundary conditions for the concentration fields are given by;

$$\begin{aligned}&C=C_w \quad \text{at } y=0,\\ &C\longrightarrow C_\infty, \qquad C_p\longrightarrow C_\infty \quad \text{as } y\longrightarrow\infty.\end{aligned} \tag{2.24}$$

Now define the non-dimensional fluid phase concentration $\phi(\eta)$ and particle phase concentration $\phi_p(\eta)$ as

$$\phi(\eta)=\frac{C-C_\infty}{C_{w-C_\infty}}, \qquad \phi_p(\eta)=\frac{C_p-C_\infty}{C_{w-C_\infty}}. \tag{2.25}$$

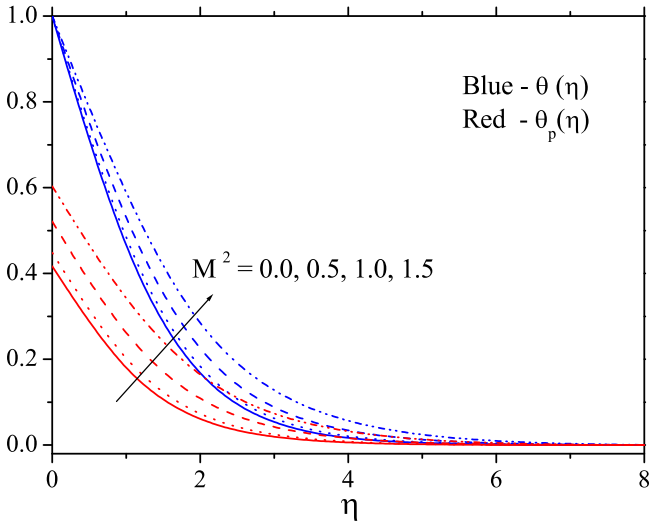

Fig. 2. The influence of M^2 on temperature profile.

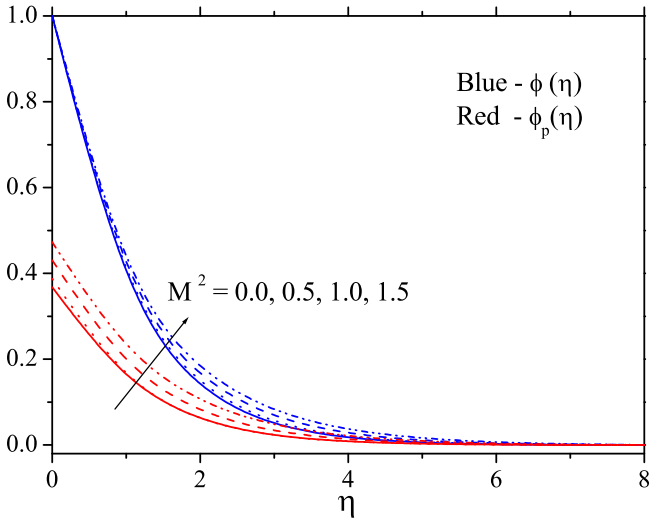

Fig. 3. The influence of M^2 on concentration profile.

Substituting (2.25) into (2.22) and (2.23), we obtain the following non-linear ordinary differential equations

$$\phi''(\eta) + Sc\left\{\begin{array}{c}\phi'(\eta) f(\eta) - f'(\eta)\phi(\eta) \\ +\beta_c l\left[\phi_p(\eta) - \phi(\eta)\right] - K\phi(\eta)\end{array}\right\} + Sr\theta''(\eta) = 0, \tag{2.26}$$

$$\phi_p'(\eta) F(\eta) - F'(\eta)\phi_p(\eta) + \beta_c\left[\phi(\eta) - \phi_p(\eta)\right] = 0. \tag{2.27}$$

With boundary conditions

$$\begin{aligned}&\phi(\eta) = 1 \quad \text{at } \eta \to 0\\ &\phi(\eta) = 0, \qquad \phi_p(\eta) = 0 \quad \text{as } \eta \to \infty,\end{aligned} \tag{2.28}$$

where $Sc = \nu/D_m$—Schmidt number, $\beta_c = 1/b\tau_c$—fluid particle interaction parameter for concentration, $K = K^*(C_w - C_\infty)/\nu$ and $Sr = D_m K_t(C_w - C_\infty)/T_m(T_w - T_\infty)$—Soret number.

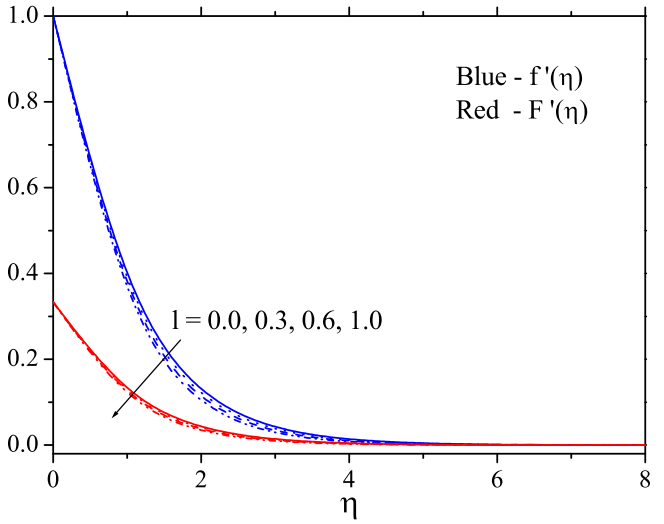

Fig. 4. The influence of l on velocity profile.

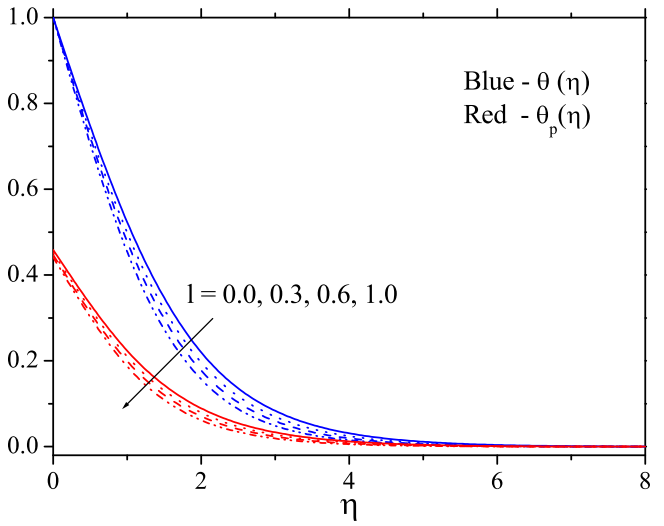

Fig. 5. The influence of l on temperature profile.

The quantities of practical interest are the skin friction coefficient, local Nusselt number and local Sherwood number and are defined as;

$$C_f = \frac{\tau_w}{\rho u_w^2}, \qquad Nu = \frac{x q_w}{k(T_w - T_\infty)} \quad \text{and} \quad Sh = \frac{x j_w}{D_m(C_w - C_\infty)}, \tag{2.29}$$

here, τ_w is the surface shear stress, q_w is the surface heat flux and j_w is the mass flux, which are given by

$$\tau_w = \mu \left(\frac{\partial u}{\partial y}\right)_{y=0}, \qquad q_w = -k \left(\frac{\partial T}{\partial y}\right)_{y=0} \quad \text{and} \quad j_w = -D_m \left(\frac{\partial C}{\partial y}\right)_{y=0}. \tag{2.30}$$

Using the similarity transformations, we obtain,

$$\sqrt{Re_x} C_f = f''(0), \qquad \frac{1}{\sqrt{Re_x}} Nu = -\theta'(0) \quad \text{and} \quad \frac{1}{\sqrt{Re_x}} Sh = -\phi'(0) \tag{2.31}$$

where $Re_x = \frac{u_w x}{\nu}$ is the local Reynolds number.

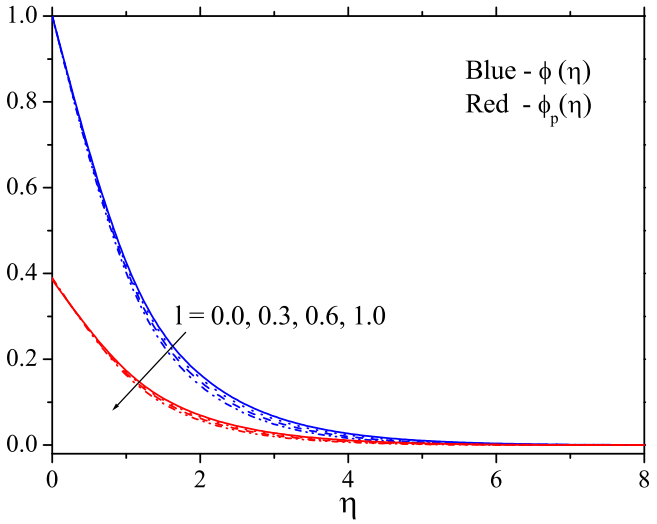

Fig. 6. The influence of l on concentration profile.

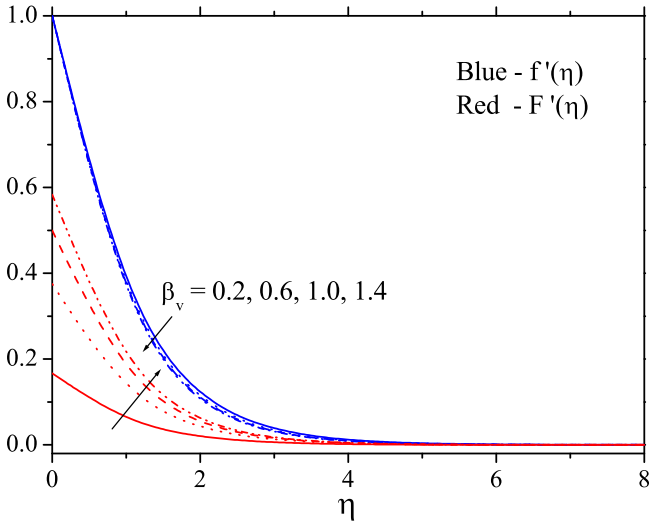

Fig. 7. The influence of β_v on velocity profile.

3. Numerical method and validation

The reduced set of non-linear ordinary differential equations is solved numerically using Shooting method along with fourth–fifth order Runge–Kutta-Fehlberg integration scheme. In algebraic package Maple, the Shooting method is implemented as an algorithm called 'shoot'. This algorithm in Maple has been well tested for its accuracy and robustness and this has been used to solve a wide range of non-linear problems. The more information regarding the 'shoot' algorithm can be found in Meade et al. [32]. It is most important to choose an appropriate finite value of η_∞. In this method, a suitable finite value of η_∞ is considered as η_8 in such way that the boundary conditions defined at infinity satisfies asymptotically. In addition, the relative error tolerance to 10^{-6} is considered for convergence and the step size is chosen as $\Delta\eta = 0.001$.

In order to validate and verify the accuracy of the applied numerical scheme, results of $-\theta'(0)$ for various values of Pr in the case of $M^2 = l = R = D_f = 0$ are compared with those reported by Grubka and Bobba [3], Ishak et al. [33] and El-Aziz [34]. The comparisons are shown in Table 1 and it is witnessed that the solutions are in very good agreement for all the considered values of parameters.

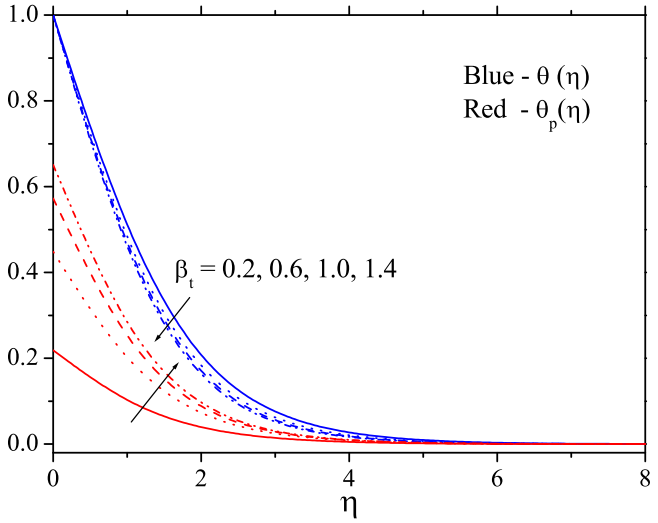

Fig. 8. The influence of β_t on temperature profile.

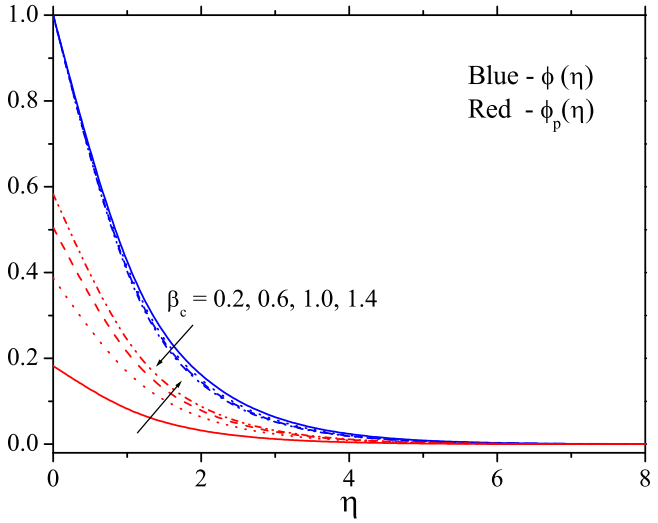

Fig. 9. The influence of β_c on concentration profile.

Table 1
Comparison results for local Nusselt number $-\theta'(0)$ with $M^2 = l = R = D_f = 0$.

Pr	Grubka et al. [3]	Ishak et al. [33]	El-Eziz [34]	Present study
0.72	0.8086	0.8086	0.80873	0.80863
1.0	1.0000	1.0000	1.00000	1.00000
3.0	1.9237	1.9237	1.92368	1.92367
10	3.7207	3.7207	3.72067	3.72067
100	12.294	12.2941	12.29408	12.29408

4. Results and discussion

To get a clear insight into the physical situation of the present problem, numerical values for velocity, temperature and concentration profile for both fluid and particle phases are computed for different values of dimensionless

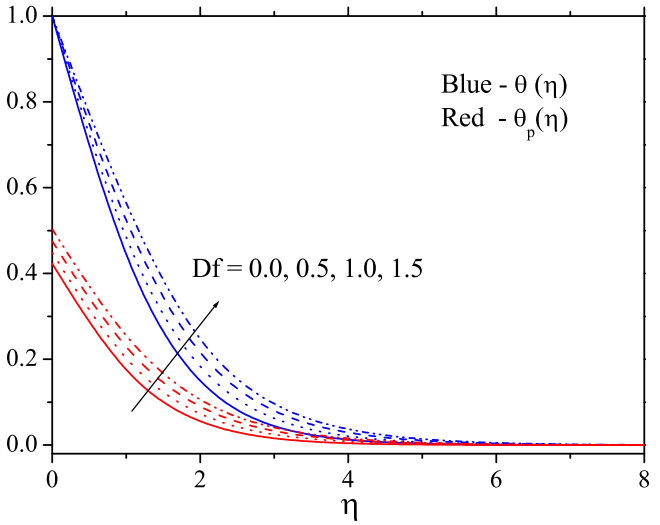

Fig. 10. The influence of *Df* on temperature profile.

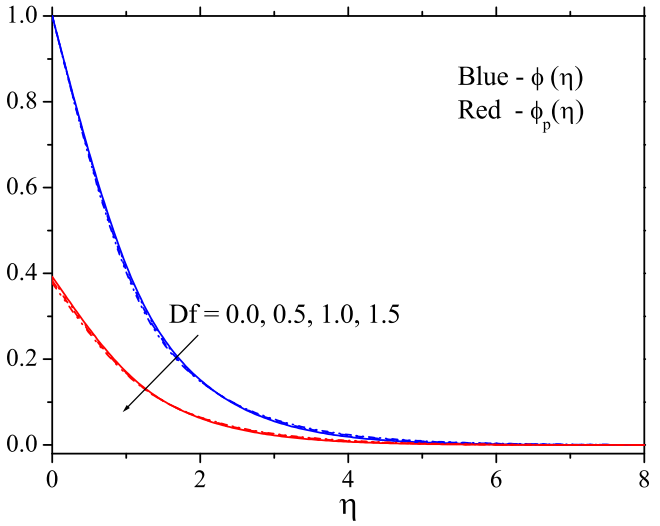

Fig. 11. The influence of *Df* on concentration profile.

parameters using the method described in the previous section. The numerical results are tabulated and displayed with the graphical illustrations. It is worth to mention that, we can recover the ordinary fluid problem by giving $l = 0$.

Figs. 1–3 show the influence of magnetic parameter on dimensionless velocity, temperature and concentration profiles of both fluid and particle phase respectively. The velocity of the fluid and particle phase decreases with an increase of the magnetic parameter. Application of the transverse magnetic field will result in a resistive type force (Lorentz force) similar to the drag force which tends to retard the fluid flow in both the phases and thus reducing its velocity. The momentum boundary layer thickness decreases with an increase in the magnetic parameter. The magnetic field can control the flow characteristics. Further, the dimensionless temperature and concentration distributions increase with an increase in the magnetic parameter for both the fluid and particle phase. The results reveal that the magnetic parameter influences the transport phenomena significantly.

Figs. 4–6 depict the effect of mass concentration of dust particle on velocity, temperature and concentration distributions for both the phases. The drag force between the fluid and particle phase is increased by increasing the mass concentration of dust particles. As a result, the momentum of the fluid retards rapidly. Consequently, the dust phase velocity becomes smaller, since the dust phase is being dragged along with the fluid. As the number of dust

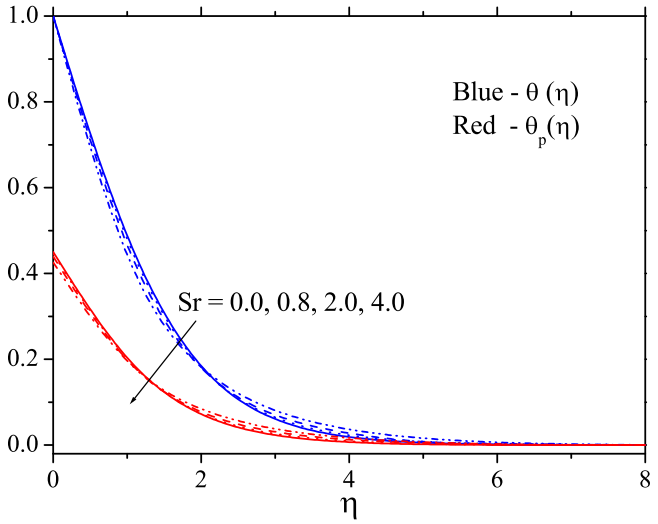

Fig. 12. The influence of *Sr* on temperature profile.

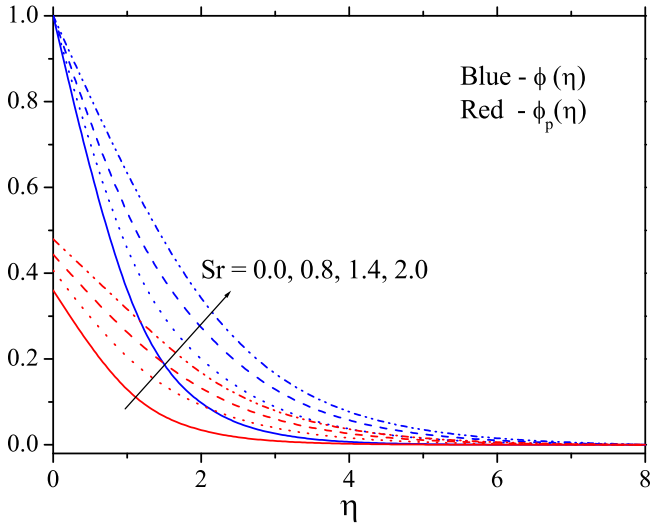

Fig. 13. The influence of *Sr* on concentration profile.

particles increase, the individual particles will receive less energy from the fluid phase. Thus, the thermal boundary layer is thin for both fluid and dust phase. This is responsible for the reduction in concentration boundary layer of both the phases.

Figs. 7–9 respectively show the effect of fluid-particle interaction parameter β_v, β_t and β_c on velocity, temperature and concentration profiles for both fluid and dust phase. These graphs illustrate that the particle phase velocity, temperature and concentration profiles increases significantly with increasing values of β_v, β_t and β_c respectively, whereas this phenomenon is quite opposite for the fluid phase throughout the boundary layer.

Figs. 10 and 11, show the Dufour effect on fluid and dust phase temperature and concentration profiles respectively. We can clearly observe from these figures that, an increase in Dufour number increases the energy flux due to a concentration gradient. This in turn will enhance the temperature of fluid and dust phase in the boundary layer. The concentration and its associated boundary layer thickness decreased by strengthening the Dufour number in the vicinity of the sheet and this trend is quite opposite at far away distance from the sheet.

The dimensionless temperature and concentration profiles for different values of Soret number are presented in Figs. 12 and 13 respectively for both fluid and dust phase. The Soret number is the ratio of the temperature

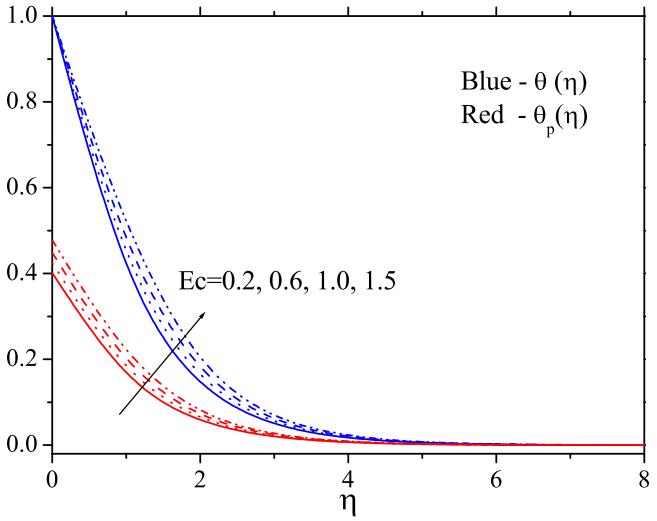

Fig. 14. The influence of *Ec* on temperature profile.

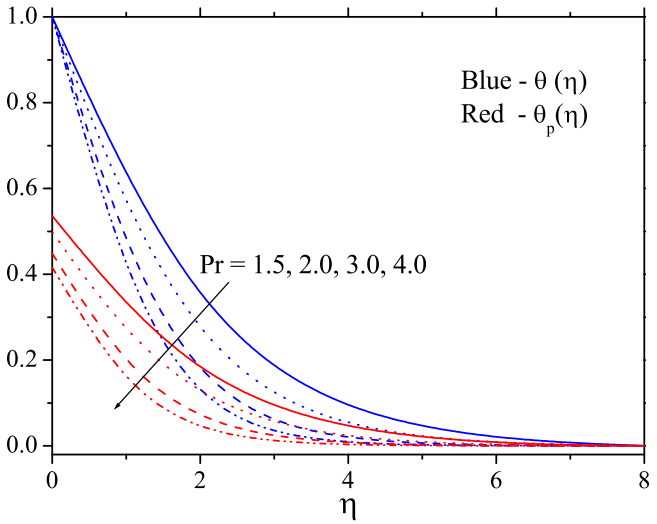

Fig. 15. The influence of *Pr* on temperature profile.

difference to the concentration difference and vice versa for the Dufour number. Hence, the opposite behaviour on the temperature and concentration for both phases are noted by increasing in Soret and Dufour numbers. In Soret effect, the temperature gradient creates the mass flux. Due to this, the temperature and its associated boundary layer thickness decrease as Soret number varies. The Soret number increases the mass diffusion; consequently, the rate of mass transfer from the surface becomes stronger. Hence, the concentration distribution is larger in both fluid and particle phase for higher values of *Sr* as shown in Fig. 13.

Figs. 14 and 15 depict the behaviour of Eckert number and Prandtl number on the temperature profile of both fluid and dust phases. Eckert number expresses the relationship between the kinetic energy in the flow and the enthalpy. It embodies the conversion of kinetic energy into internal energy by work done against the viscous fluid stresses. The greater viscous dissipative heat causes a rise in the temperature and thermal boundary layer thickness for both fluid and particle phase. Besides, as expected, the temperature distribution in the boundary layer is decreased by increasing the Prandtl number. This is due to the fact that, the Prandtl number is the ratio of viscous diffusivity to the thermal diffusivity. The thermal diffusivity reduces by an increase in the Prandtl number. As a result, the thermal boundary thickness for both fluid and dust phase decreases rapidly.

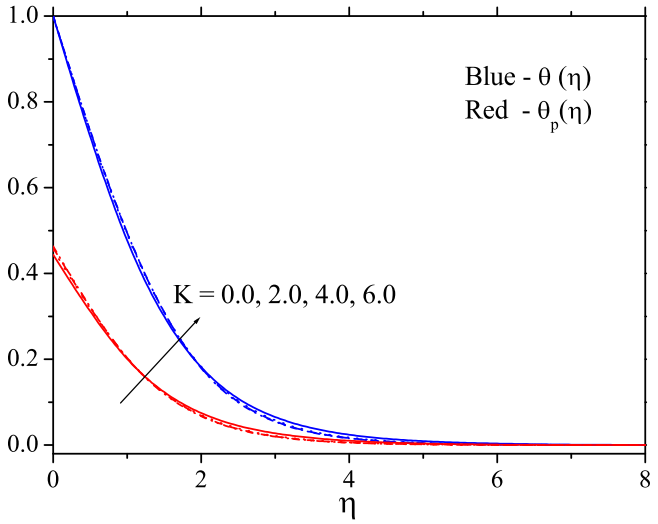

Fig. 16. The influence of K on temperature profile.

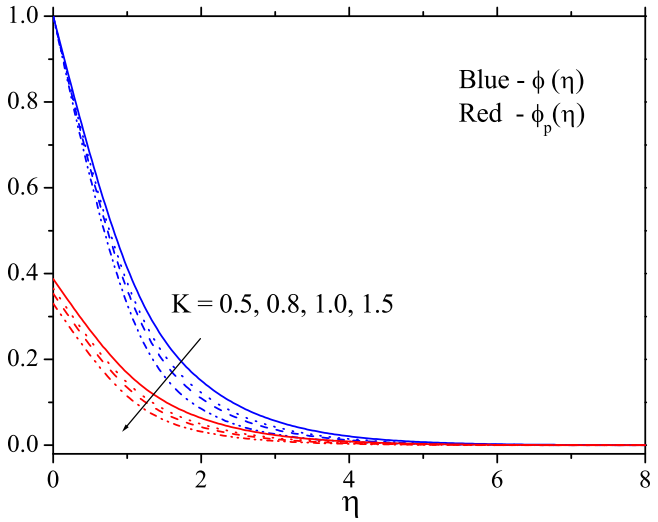

Fig. 17. The influence of K on concentration profile.

The responses of both fluid and particle phase temperature and concentration profile with the variation of chemical reaction parameter is portrayed in Figs. 16 and 17. The temperature distribution of the fluid and particle phase gradually increases from lower value to the higher value only when the strength of the rate of chemical reaction parameter increases. Besides, there is a reduction in both fluid and particle phase concentration distribution is accompanied by strengthening the chemical reaction. This shows that the diffusion rates can be tremendously altered by chemical reactions.

Figs. 18 and 19 depict the effect of radiation parameter and Schmidt number on temperature and concentration profile for dust and fluid phase respectively. The temperature and its corresponding boundary layer (both fluid and dust phase) thickness increase by increasing thermal radiation parameter. Further, it depicts that, the thermal boundary layer thickness is higher in the presence of thermal radiation effect ($R \neq 0$) than its absence ($R = 0$). The concentration (fluid and dust phase) decreases when the values of Schmidt number are increased. This is because of the fact that by increasing the Schmidt number, the mass diffusivity decreases and solute boundary layer decreases in both phases.

Finally, the variation of skin friction coefficient and Nusselt number profiles for different values of M^2, Ec, l, Sr, Df, Sc, Pr, β_v, β_t and β_c are presented in Tables 2 and 3. The skin friction co-efficient at the surface is

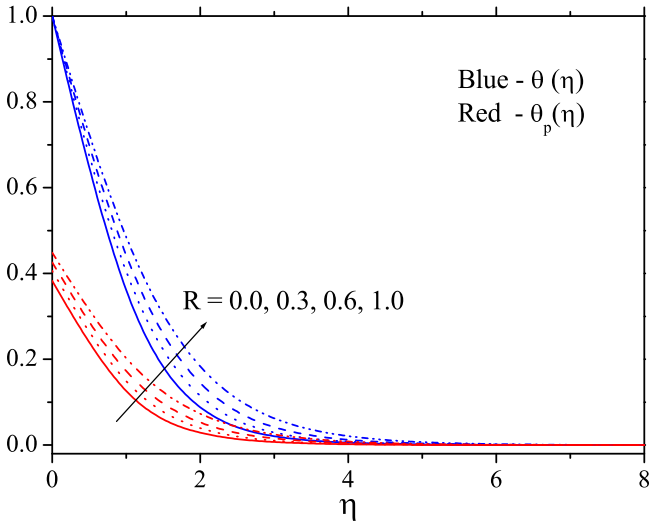

Fig. 18. The influence of R on temperature profile.

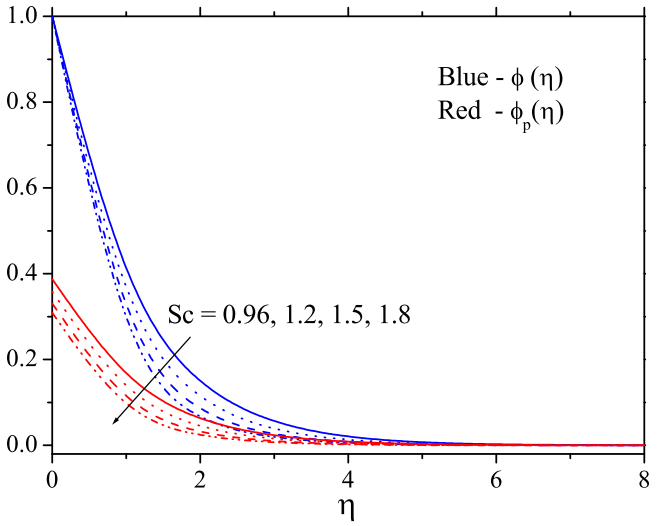

Fig. 19. The influence of Sc on concentration profile.

decreases with increasing values of l and β_v and increases for increasing value of M. The Nusselt number increases with the increasing values of l, Pr, Sr and β_c while this phenomenon is opposite for increasing values of M, Ec, Df, Sc, C and β_v. Moreover, for increasing values of Sc, Sr, Ec, β_t and l, the Sherwood number increases, where as this phenomenon is opposite for the increasing values of M, Sr, Pr, β_c and β_v.

5. Conclusion

Two-phase flow, heat and mass transfer of a dusty fluid with Soret and Dufour's effect over a stretching surface in the presence of a magnetic field, thermal radiation, and chemical reaction have been studied numerically. The results pertaining to the present study are listed below,

- Due to strengthening magnetic field and mass concentration of dust particles, momentum boundary layer decreases rapidly for both the phases.
- The temperature and concentration boundary layer thickness decreases via larger mass concentration of dust particles.

Table 2
Numerical results of $f''(0)$, $-\theta'(0)$ and $-\varphi'(0)$ for different values of l, M^2, β_v, β_t and β_c.

l	M^2	β_v	β_t	β_c	$f''(0)$	$-\theta'(0)$	$-\phi'(0)$
0					1.118042	0.866430	1.129051
0.5					1.190244	0.962881	1.190236
1					1.258310	1.050411	1.248564
	0.2				1.098509	1.009569	1.198858
	0.4				1.151821	0.982472	1.193772
	0.6				1.235586	0.939711	1.186201
		1			1.224749	0.945677	1.187266
		1.5			1.244994	0.935766	1.185630
		2			1.258309	0.929332	1.184599
			1		1.190244	0.961034	1.218484
			1.5		1.190244	0.959533	1.241297
			2		1.190244	0.958514	1.256728
				1	1.190244	1.005486	1.183982
				1.5	1.190244	1.039215	1.178988
				2	1.190244	1.061695	1.175641

Table 3
Numerical results of $f''(0)$, $-\theta'(0)$ and $-\phi'(0)$ for different values of Sr, Df, Sc, Ec and Pr.

Sr	Df	Sc	Ec	Pr	$f''(0)$	$-\theta'(0)$	$-\phi(0)$
0					1.190244	0.957029	1.285480
0.5					1.190244	0.971926	1.043719
1					1.190244	0.987759	0.789115
	0				1.190244	1.025836	1.180844
	0.5				1.190244	0.865880	1.204776
	1				1.190244	0.696857	1.230304
		0.96			1.190244	0.962881	1.190236
		1.5			1.190244	0.936953	1.576235
		3			1.190244	0.879591	2.373818
			0		1.190244	1.186849	1.153226
			0.4		1.190244	0.962881	1.190236
			0.8		1.190244	0.738914	1.227246
				3	1.190244	0.962881	1.190236
				6	1.190244	1.453590	1.116598
				7.2	1.190244	1.607466	1.091866

- Increasing values of Dufour and Eckert number, magnetic parameter and radiation parameters show enhancement in the temperature and thermal boundary layer thickness for both fluid and dust phases.
- The concentration profile decreases by increasing chemical reaction parameter and Schmidt number.
- The momentum, thermal and solutal boundary layer is lower in the particle phase than that of fluid phase.
- The technology of suspending dust particles into the working fluids to control the flow, thermal and solute characteristics is better suited in many industrial and manufacturing processes.
- The governing equations for an ordinary viscous fluid can be recovered when $l = 0$.

Acknowledgment

One of the authors, B.J. Gireesha wishes to express his gratitude to University Grants Commission, New Delhi, India No. F 5-110/2014 (IC) for the financial support under Raman Fellowship 2014–2015 for pursuing this work.

References

[1] Sakiadis BC. Boundary layer behavior on continuous solid surface. AIChE J 1961;7:26–34.
[2] L.J. Crane. Flow past a stretching sheet. Z Angew Math Phys 1970;21:645–7.

[3] Grubka LJ, Bobba KM. Heat transfer characteristics of a continuous stretching surface with variable temperature. J Heat Transfer 1985;107:248–50.
[4] Dursunkaya Z, Worek WM. Diffusion-thermo and thermal-diffusion effects in transient and steady natural convection from vertical surface. Int J Heat Mass Transfer 1992;35(8):2060.
[5] Anghel M, Takhar HS, Pop I. Dufour and Soret effects on free convection boundary-layer over a vertical surface embedded in a porous medium. Studia Univ Babeş-Bolyai Math 2000;11–22. XLV.
[6] Postelnicu A. Influence of magnetic field on heat and mass transfer by natural convection from vertical surfaces in porous media considering Soret and Dufour's effect. Int J Heat Mass Transfer 2004;47(6):1467–72.
[7] Hayat T, Mustafa M, Pop I. Heat and mass transfer for Soret and Dufour's effect on mixed convection boundary layer flow over a stretching vertical surface in a porous medium filled with a viscoelastic fluid. Commun Nonlinear Sci Numer Simul 2010;15(5):1183–96.
[8] Beg A, Bakier AY, Prasad VR. Numerical study of free convection magnetohydro-dynamic heat and mass transfer from a stretching surface to a saturated porous medium with Soret and Dufour effects. Comput Mater Sci 2009;46(1):57–65.
[9] Aziz MAE. Thermal-diffusion and diffusion-thermo effects on combined heat and mass transfer by hydromagnetic three-dimensional free convection over a permeable stretching surface with radiation. Phys Lett A 2008;372(3):263–72.
[10] Pal D, Chatterjee S. Mixed convection magnetohydrodynamic heat and mass transfer past a stretching surface in a micropolar fluid-saturated porous medium under the influence of Ohmic heating, Soret and Dufour effects. Commun Nonlinear Sci Numer Simul 2011;16(3):1329–46.
[11] Makinde OD, Olanrewaju PO. Unsteady mixed convection with Soret and Dufour effects past a porous plate moving through a binary mixture of chemically reacting fluid. Chem Eng Commun 2011;198:920–38.
[12] Olanrewaju PO, Makinde OD. Effects of thermal diffusion and diffusion thermo on chemically reacting MHD boundary layer flow of heat and mass transfer past a moving vertical plate with suction/injection. Arab J Sci Eng 2011;36(8):1607–19.
[13] Pal D, Mondal H. Effects of Soret, Dufour, chemical reaction and thermal radiation on MHD non-Darcy unsteady mixed convective heat and mass transfer over a stretching sheet. Commun Nonlinear Sci Numer Simul 2011;16(4):1942–58.
[14] Pal D, Mondal H. MHD non-Darcian mixed convection heat and mass transfer over a non-linear stretching sheet with Soret–Dufour effects and chemical reaction. Int Commun Heat Mass Transfer 2011;38(4):463–7.
[15] Kandasamy R, Hayat T, Obaidat S. Group theory transformation for Soret and Dufour effects on free convective heat and mass transfer with thermophoresis and chemical reaction over a porous stretching surface in the presence of heat source/sink. Nucl Eng Des 2011;241(6):2155–61.
[16] Postelnicu A. Influence of chemical reaction on heat and mass transfer by natural convection from vertical surfaces in porous media considering Soret and Dufour effects. Heat Mass Transfer 2007;43(6):595–602.
[17] Das K. Effect of chemical reaction and thermal radiation on heat and mass transfer flow of MHD micropolar fluid in a rotating frame of reference. Int J Heat Mass Transfer 2011;54:3505–13.
[18] Mansor MA, El-Anssary NF, Aly AM. Effect of chemical reaction and thermal stratification on MHD free convective heat and mass transfer over a vertical stretching surface embedded in a porous media considering Soret and Dufour numbers. Chem Eng J 2008;145:340–5.
[19] Makinde OD, Zimba K, Beg OA. Numerical study of chemically-reacting hydromagnetic boundary layer flow with Soret/Dufour effects and a convective surface boundary condition. Int J Therm Environ Eng 2012;4:89–98.
[20] Chamkha AJ, EL-Kabeir . Unsteady heat and mass transfer by MHD mixed convection flow over an impulsively stretched vertical surface with chemical reaction and Soret and Dufour effects. Chem Eng Commun 2013;200(9):1220–36.
[21] Gireesha BJ, Mahanthesh B, Rashidi MM. MHD boundary layer heat and mass transfer of a chemically reacting Casson fluid over a permeable stretching surface with non-uniform heat source/sin. Int J Ind Math 2015;7:14.
[22] Saffman PG. The stability of a laminar flow of a dusty gas. J Fluid Mech 1962;13(3):120–8.
[23] Chamkha AJ. Effects of particulate diffusion on the compressible boundary-layer flow of a two-phase suspension over a horizontal surface. J Fluids Eng 1998;120:146–51.
[24] Chamkha AJ. Hydromagnetic flow and heat transfer of a particulate suspension over a non-isothermal surface with variable properties. Int J Fluids Mech Res 2000;27:2–4.
[25] Chamkha AJ, Ramadan HM. Analytical solutions for free convection flow of a particulate suspension past an infinite vertical surface. Internat J Engrg Sci 1998;36(1):49–60.
[26] Vajravelu K, Nayfeh J. Hydromagnetic flow of a dusty fluid over a stretching sheet. Internat J Non-Linear Mech 1992;27:937–45.
[27] Makinde OD, Chinyoka T. MHD transient flows and heat transfer of dusty fluid in a channel with variable physical properties and Navies slip condition. Comput Math Appl 2010;60:660–9.
[28] Attia HA, Abbas W, Abdeen MAM. Ion slip effect on unsteady Couette flow of a dusty fluid in the presence of uniform suction and injection with heat transfer. J Braz Soc Mech Sci Eng 2015; http://dx.doi.org/10.1007/s40430-015-0311-y.
[29] Gireesha BJ, Roopa GS, Bagewadi CS. Effect of viscous dissipation and heat source on flow and heat transfer of a dusty fluid over unsteady stretching sheet. Appl Math Mech 2012;30(8):1001–14.
[30] Gireesha BJ, Mahanthesh B, Gorla RSR. Suspended particle effect on nanofluid boundary layer flow past a stretching surface. J Nanofluids 2014;3:267–77.
[31] Gireesha BJ, Mahanthesh B, Gorla RSR, Manjunatha PT. Thermal radiation and Hall effects on boundary layer flow past a non-isothermal stretching surface embedded in porous medium with non-uniform heat source/sink and fluid-particle suspension. Heat Mass Transfer 2015; http://dx.doi.org/10.1007/s00231-015-1606-3.
[32] Meade DB, Haran BS, White RE. The shooting technique for the solution of two-point boundary value problem. Maple Technol 1996;3:85–93.
[33] Ishak A, Nazar R, Pop I. Boundary layer flow and heat transfer over an unsteady stretching vertical surface. Meccanica 2009;44:369–75.
[34] Aziz MA. Mixed convection flow of a micropolar fluid from an unsteady stretching surface with viscous dissipation. J Egyptian Math Soc 2013;21:385–94.